Kinetics of superconductivity destruction by current in thin films

Yu. M. Ivanchenko, P. N. Mikheenko, and V. F. Khirnyĭ

Donetsk Physicotechnical Institute, Ukrainian Academy of Sciences
(Submitted 8 January 1980; resubmitted 30 July 1980)
Zh. Eksp. Teor. Fiz. **80**, 171–182 (January 1981)

Current-voltage characteristics are used to investigate the kinetics of superconductivity destruction in soft-superconductor thin films made by sputtering Al, Sn, and In on cover glasses. The properties of the metastable dissipative states that arise only after the transport current exceeds the critical value and after its subsequent decrease to a value below the critical current are considered in detail. The lower limit of existence of dissipative states that are metastable with respect to voltage near the section where the site of superconductivity destruction is indicated. The nature of the hysteresis of the current-voltage characteristics is elucidated on the basis of the heat-conduction equation. A method is proposed for calculating the superheat temperature of films through which transport current flows.

PACS numbers: 73.60.Ka, 74.30. – e

INTRODUCTION

An investigation of the current-voltage characteristics (CVC) of soft thin-film superconductors made of Al, Sn, and In has shown that a critical current $I_c \ll I_p$ (I_p is the Ginzburg pair-breaking current[1]) destroys the superconductivity in them locally, and superconducting and nonsuperconducting zones alternate along the current flow.[2-4] It is important that despite the heat release, the superconductivity-destruction sites do not extend over the entire sample, even at currents much higher than I_c. This circumstance makes the model described in Ref. 5 unsuitable for the understanding of the superconductivity destruction in thin films.

We report here an investigation of the kinetics of superconductivity destruction in such film, using an analysis of their CVC. We show that the hysteresis of the CVC is of thermal origin, and that the formation of the CVC proceeds in several stages, the most important of which is the formation of a special dissipative state that preserves part of the superconducting current and contains simultaneously an inhomogeneous electric field. A method is proposed for determining the local temperature in the superconductivity-destruction site.

EXPERIMENTAL PART

We evaluate in this paper the results of an investigation of a large number of thin-film superconductors made of Al, Sn, and In. More than 50 samples were produced. The principal parameters of some of them are listed in Table I, where the following notation is used: W is the width and d the thickness of the sample; ρ is the resistivity in the normal state at 4.2 K, l_e is the effective mean free path of the electrons, $\varkappa$ is the Ginzburg-Landau parameter, and T_c is the critical temperature. The spread in the values of ρ, l_e, and $\varkappa$ is brought about by the inaccuracy in the determination of d. The method of preparing the sample, whereby the parameter $\varkappa$ ranged from 0.14 to 400, the procedure for measuring the CVC, the determination of T_c and I_c, as well as the cryogenic and measuring equipment were described earlier in Ref. 4. Although most samples were type-II superconductors, their CVC were nevertheless not different qualitatively from those of films with $\varkappa < 1/\sqrt{2}$. Therefore the entire reasoning in the article applies equally the superconductors with arbitrary $\varkappa$ (with the exception of the quantitative analysis for a particular sample).

TABLE I. Most important parameters of investigated samples.

Sample No.	Material	W, 10^{-6}, m	ρ, 10^{-8} Ω · m	d, 10^{2} nm	l_e, Å	$\varkappa$	T_c, K
1	In	0.3	3.3–4.1	1.6–2	317–396	0.5–0.6	3.6
7	Sn	0.3	45–81	0.5–0.9	20–36	7.3–13.1	4.14
23	Al	0.1	15.2–21.5	1.2–1.6	42–60	1.9–2.7	1.31
47	Sn *	0.47	14–17	1.6–2.0	94–118	2.4–2.9	3.8

*Cylindrical sample.

Figure 1 shows the experimental CVC of an indium film (sample 1). It is seen from the figure that four sites of superconductivity destruction were produced in this film at currents I_M, I_N, I_K, and I_φ. This CVC is complicated in form, but can be resolved into simple components (fragments), each of which constitutes the CVC of one of the destruction sites. Inasmuch as these sites form a series circuit for the transport current, the CVC of the entire sample is the sum (with respect to voltage) of these fragments. Individual fragments can be singled out by two methods, one of which is demonstrated in Fig. 2 for sample 1. It consists of a successive graphic subtraction of the CVC by the follow-

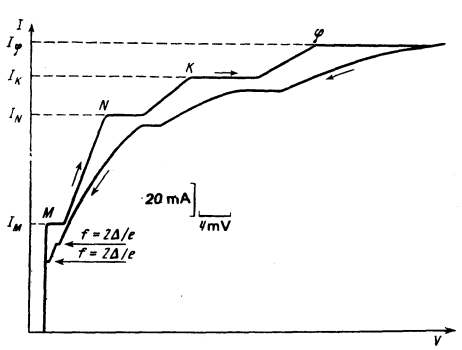

FIG. 1. General form of CVC of thin In film, sample 1; T_0 = 2.9 K.

 0038-5646/81/010086-06$02.40

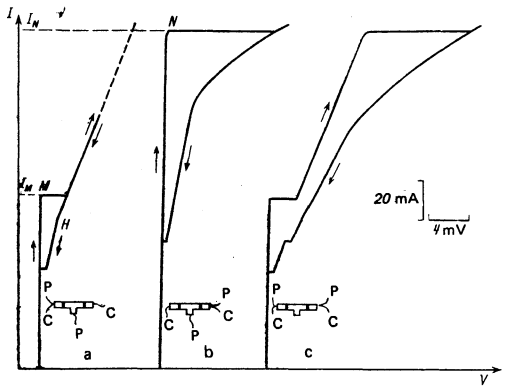

FIG. 2. Resolution of complete CVC into fragments, sample 1; $T_0 = 2.5$ K.

ing procedure: The first fragment, shown in Fig. 2(a), is obtained when the CVC of the film is plotted with the current varied in a region somewhat above I_M but below I_N (see Fig. 1). If we plot now the CVC with the current varied above I_N but below I_K [Fig. 2(c)] and subtract from this plot (with respect to voltage, i.e., by leftward horizontal shift) the first fragment continued by a straight line [the continuation is shown dashed in Fig. 2(a)] until the corresponding value of the current is reached, we obtain the characteristic connected with the second destruction site, i.e., the second fragment, which is shown in Fig. 2(b). The third and succeeding fragments can be similarly obtained if the characteristic in the forward direction is linear between the horizontal steps. Wherever this condition is not satisfied a second method of separation into fragments was used: The CVC of film sections with more than one superconductivity-destruction sites were obtained directly with the aid of several potential leads constructed in the form of a comb. This procedure was used, for example, to investigate the Sn film (sample 7). The insets of Fig. 2 show those positions of the potential leads (marked by the letter "*P*") which would make it possible to plot the CVC fragments of the In sample 1 by the second method. The wide solid lines show symbolically the superconductivity-destruction sites; the letter "*C*" marks the current leads. As a rule, for the first two or three fragments (and in individual cases up to five) the resolution by the first and second methods led to identical characteristics.

DISCUSSION OF THE PROCESS OF SUPERCONDUCTIVITY DESTRUCTION BY A CURRENT

§1. Analysis of formation of CVC fragment

The process of formation of the CVC fragment can be divided into several stages.

The first stage is nondissipative, when the current rises from zero to the value I_1 needed for the entry of one vortex (or of one flux tube in the case of a type-I superconductor).

The instant when the current reaches this critical value coincides with the start of the second stage of CVC formation. Since the investigated films are soft superconductors and there is practically no volume pinning in them, the entering vortex (or flux tube), overcoming the viscous-friction force, begins immediately to move under the influence of the Lorentz force, in a direction perpendicular to the transport current, striving to cross the film along the shortest path from the entry point. Owing to the long-range interaction between vortices in thin films with $d \ll \lambda$ (Ref. 6) (λ is the depth of penetration of the magnetic field), the height of the barrier to the entry of the second vortex is increased, and to enable more than one vortex to be present in the film simultaneously, the current must be increased somewhat. The motion of the vortices gives rise to a voltage[1] $V = \Phi_0/c\tau_L(I)$, where Φ_0 is the magnetic-flux quantum, $\tau_L(I)$ is the time for the vortices to traverse the distance between them, and c is the speed of light. The work performed by the external source to overcome the friction is converted into heat that is dissipated along the vortex trajectory.

So long as $\tau_L(I) > \tau_0$ (τ_0 is the time of temperature relaxation to the equilibrium value), the CVC is reversible, i.e., it contains no hysteresis sections. Thus, the second stage of CVC formation is the passage through reversible dissipative section observed in the interval between the current I_1, at which one vortex penetrates into the film, to I_c, when τ_L reaches the value τ_0. For the investigated films, this section of the characteristic, at $T < 0.98T_c$, usually corresponded to a current equal to several percent of I_c, and expanded to several percent only in the immediate vicinity of T_c. For the characteristic shown in Fig. 1, I_c is equal to one of the values I_M, I_N, I_K, or I_φ, depending on the selected fragment. The hardly noticeable roundoff near one of these current values is in fact the section from I_1 to I_c. It is noteworthy that the CVC formed during the second stage is essentially nonlinear. We shall not analyze this section in greater detail here.

The third stage of CVC formation sets in when the current reaches the value I_c. Inasmuch as in this case $\tau_L \approx \tau_0$, the temperature at the locations where the vortices move does not manage to relax to the thermostat temperature, and the sample is locally heated along the vortex trajectory. The temperature rise, however, lowers the barrier to the entry of vortices, and consequently increases their linear density, i.e., leads to further heating. A temperature instability thus develops and terminates at the instant when the linear density of the vortices reaches a critical value at which the vortex cores begin to overlap. The instability development time is very short, of the order of 10^{-8} to 10^{-11} sec, so that the transition region appears on the CVC as a horizontal voltage step. After passing through this step it is no longer possible to return to states characteristic of the second or first stage, even if the current is decreased below I_1. The reason is that the superconducting film goes over into a new metastable nonequilibrium state, which it can leave only by finite excitation of duration longer than τ_0 (Ref. 4), since our system, even when brought by a voltage pulse to a state with $V = 0$, must manage to give up the excess heat to the thermostat during the time of action of the pulse. The new state produced after the step is char-

acterized by a stationary local distribution of the temperature along the current-flow direction, with a maximum located on the line along which the vortices move at lower values of the current. It is simplest to assume that the temperature is constant along this line, and calculation shows (see § 3) that this assumption agrees well with the experimental data. It turns out then that the temperature T_m at the center of the SDS (superconductivity-destruction site) exceeds, after passage through the step, the value of T_c at the given current. As a consequence, a small normal region is produced in the film. When the current is decreased at the point H [Fig. 2(a)], T_m becomes equal to T_c and the normal region vanishes. From the linearity of the CVC section of the first fragment above the point H it follows that for this fragment the contribution of the normal region to the dissipation is negligible. The nonlinearity of this section on the succeeding fragments is clearly seen.

Below the point H is located the second linear section of the CVC, which joins the first at an angle somewhat different from 180°. This section is of particular interest, since the film is there is a metastable superconducting dissipative state (MSDS). Let us analyze it in greater detail.

It is obvious that a homogeneous electric field in a superconductor is not compatible with superconductivity, since it leads to an accelerated motion of the Cooper pairs, and hence to their decay when critical velocities are reached. On the other hand a nonuniform field is perfectly compatible with superconductivity, since a Cooper pair that comes under the influence of the field can jump through it without reaching critical velocity. In this case all the dissipative processes are connected with normal excitations in the region where the electric field acts. Such a state, however, cannot be stationary, since the Cooper-pair current short-circuits the region with the electric field, and unless E is maintained by some artificial means, the field will vanish. To produce a metastable state it is therefore necessary that the Cooper pairs decay in the region where the field acts. Then, in addition to the dissipation due to normal excitation, an additional dissipation mechanism appears and apparently assumes the principal role at fields that are not too strong.

In fact, the electrons in the bound pair, accelerated in the electric field over a distance l, acquire an additional energy δe equal to eEl (e is the electron charge). If $\delta\varepsilon$ exceeds the pair-binding energy 2Δ, then the pair electron, in an encounter with a defect, can become scattered and the pair is then broken. Since $eEl = eV$, it follows from this reasoning that the minimum voltage V_{min} that can be realized in the MSDS is

$$V_{min} = 2\Delta/e. \qquad (1)$$

This value of V_{min} and its temperature dependence are surprisingly well confirmed by experiments on a number of samples (see Figs. 1 and 3). Figure 3 shows the temperature dependence of the value f, referred to $2\Delta(0)/e$, of the step on the backward branch of the CVC, measured for films 1, 23, and 47 at several values of T_0. The solid line shows the temperature dependence

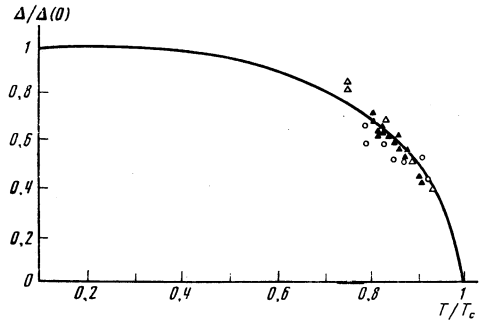

FIG. 3. Value of f of lowest step of the return part of the CVC, referred to $2\Delta(0)/e$. The data are shown for the following films: ▲) In (sample 1), ○) Al (sample 23, △) Sn (sample 47).

of $\Delta(T)/\Delta(0)$. The energy gap was determined from the formula $2\Delta(0)/T_c = \alpha$ where $\alpha_{Al} = 3.36$, $\alpha_{In} = 3.55$, and $\alpha_{Sn} = 3.6$.[7] The quantity $\Delta(T)$ in relation (1) should be taken at the maximum value of the local temperature $T = T_m$. The reason is that the thermal length $\lambda_T \sim 10^{-3}$ cm is the largest characteristic MSDS length. The values of f were measured in the temperature interval $T_0 \sim (0.4\text{–}0.92)T_c$. Nonetheless (see Fig. 3), in the transition to the superconducting state, T_m always remained higher than $0.75T_c$, and this determined the hysteresis of the CVC and restricted to temperature interval of the value of $\Delta(T)$ determined by measuring f.

The use of the assumption that λ_T exceeds noticeably the distance l over which an electric field exists will also play an important role in what follows. We therefore estimate l, assuming that[2)] $l \sim lE \sim l\varepsilon(T/\Delta)^{1/2}$, where l_E is the depth of penetration of the electric field into the superconductor, obtained by Artemenko and Volkov,[9] $l\varepsilon = (l_e l_i/3)^{1/2}$, where l_e is the effective elastic path and l_i is the effective inelastic relaxation length. As for the factor $(T/\Delta)^{1/2}$, it is practically equal to unity in the entire investigated temperature region.

When estimating the characteristic length $l\varepsilon$ one must take into account the following circumstances. First, in the investigated films the length[3)] l_e is determined by dimensions of the order of the sizes a of the crystallites that make up the film structure, or may even be considerably smaller because the conductivity in the normal state is connected with tunnel currents between individual granules. For most investigated samples l_e ranged from ~10 to ~100 Å. Second, l_i must be determined with allowance for the fact that when the electrons are scattered by the boundaries of the granules or crystallites, or simply by the film surface, there is a finite probability of exciting surface phonons (Rayleigh waves, see Ref. 10). In this case the main contribution to l_i is made precisely by the surface phonons.

In fact, l_i can be represented in the form a/ξ (where ξ is the probability of exciting a Rayleigh wave upon excitation with the boundary). To estimate ξ we imagine that the electron moves only along the boundary, and then the excitation lifetime τ_ε is determined by its energy relaxation via scattering with emission of two-dimensional waves, and is of the order of $\tau_\varepsilon \sim \omega_D/T^2$

(where ω_D is the Debye energy). However, the time τ_s during which the electron is located in the vicinity of the surface, where it can give up excess energy by emitting a Rayleigh phonon, is short and is of the order of λ'/v_0, where λ' is the region of localization of the wave, and v_0 is the Fermi velocity. Recognizing that $\lambda' \sim s/\omega \sim s/T$ (s and ω are the velocity and frequency of the Rayleigh sound) as well as that $\xi \sim \tau_s/\tau$, we obtain $l_i \sim av_0\omega_D/T_s$. As a result, $l\varepsilon$ is of the order of 10^{-4}–10^{-5} cm. Naturally, this is a rather rough estimate, but it is important in what follows that $l_E \ll \lambda_T$.

§2. Temperature distribution in the vicinity of the energy dissipation line

To investigate the temperature distribution in the region of superconductivity destruction, in the voltage and current intervals where the MSDS is realized, we must write down the heat-balance equation for a film sputtered on a glass substrate and in thermal contact with liquid helium. In the derivation of the appropriate equation we use the following simplifying assumptions: 1) The condition $l \ll \lambda_T$ allows us to represent the heat source by a δ function. 2) Since the thicknesses of the investigated films satisfy the condition $d \ll \lambda_T$, the variation of the temperature over the thickness can be neglected. 3) The widths of all films satisfy the inverse condition $W \gg \lambda_T$, so that a certain change in the heat balance near the edges of the films can be neglected. 4) The dissipation line is assumed straight and perpendicular to the current-flow direction. 5) The entire analysis is for one fragment without allowance for the neighboring superconductivity destruction sites.

Under these assumptions, the heat-balance equation takes the form

$$\frac{d}{dx}K(T)\frac{dT}{dx}-A(T)(T-T_0)+\delta(x)B=\rho' C\frac{\partial T}{\partial t}, \tag{2}$$

where x is the coordinate along the film length with the heat source at the point $x=0$, T_0 is the thermostat temperature, K is the thermal-conductivity coefficient referred to the film thickness, $A=(H_1+H_2)/d$ is the coefficient of heat transfer to the glass and to the liquid helium per unit length, $B=P/Wd$ (where P is the power loss in the film), ρ' is the density of the sample material, and C is the heat capacity. The first term in the left-hand side of (2) describes the propagation of the heat along the film, the second its outflow to the liquid helium and the substrate, and the third the heat released in the energy-dissipation region.

We must first investigate the process whereby the temperature fluctuations are damped, so as to obtain an expression for the time τ_0. It suffices for this purpose to consider the solution of Eq. (2) in the absence of a heat source ($B=0$), assuming that at the instant of time $t=0$ the temperature has a certain nonequilibrium distribution with $\Delta T(x)=T(x)-T_0$. If the inequality $\Delta T(x) \ll T_0$ is satisfied, the quantities K, A, and C can be regarded as constants taken at $T=T_0$. It is then easy to obtain for $\Delta T(x,t)$ the relation

$$\Delta T(x,t)=\int \frac{dx'\Delta T(x')}{2(\pi Dt)^{1/2}}\exp\left[-\frac{t}{\tau_0}-\frac{(x-x')^2}{4Dt}\right], \tag{3}$$

where $D=K/\rho' C$ and $\tau_0=\rho' C/A$. As seen from (3), the weak temperature fluctuations, on the one hand, attenuate exponentially with time via heat transfer to the helium and the glass substrate, and on the other hand diffuse spreading of the initial distribution $\Delta T(x)$ takes place along the film via the heat-conduction mechanism.

The quantity τ_0 determined from relation (3) does not depend on the temperature to which the film was heated at the initial instant of time, and tends to zero as $T_0 \to 0$. These facts are the consequence of the assumption that $\Delta T(x) \ll T_0$. At sufficiently low temperatures, under dissipation conditions, this inequality will always be violated. To estimate the relaxation time it is therefore desirable not to restrict oneself to linearization of the initial equation (2). It is impossible in the general case to obtain an analytic solution of this equation. It is more or less obvious, however, that the temperature relaxation time does not exceed the time of homogeneous relaxation.

An expression for the homogeneous relaxation time can be obtained from the definition

$$\tau_0=\frac{1}{\bar{T}-T_0}\int_0^\infty dt[T(t)-T_0], \tag{4}$$

where $T(t)$ is the spatially homogeneous solution of Eq. (2) with $B=0$, and $\bar{T}$ is temperature at $t=0$. Using Eq. (2) and the definition (4), we can reduce the equation for τ_0 to the form

$$\tau_0=\frac{1}{\bar{T}-T_0}\int_{T_0}^{\bar{T}} dT\frac{\rho'(T)C(T)}{A(T)}. \tag{5}$$

Using the data of Refs. 11–14, we find that τ_0 for all the investigated materials ranges from 10^{-8} to 10^{-11} sec, depending on the thermostat temperature T_0, on the immersion medium, and on the substrate material.

To investigate the temperature distribution in the vicinity of the superconductivity destruction site it is necessary to find a stationary solution of Eq. (2) with $B \neq 0$. Obviously, in this case $T(x)$ is an even function of x, so that it suffices to find it for $x>0$, i.e., to solve the equation

$$\frac{d}{dx}K\frac{dT}{dx}-A(T)(T-T_0)=0 \tag{6}$$

in the region $x>0$ with the boundary conditions

$$2K\frac{dT}{dx}\Big|_{x=0}=-B, \quad \lim_{x\to\infty}T(x)=T_0. \tag{7}$$

Equation (6) with allowance for relations (7) is transformed into

$$\left[K(T)\frac{dT}{dx}\right]^2=2\int_{T_0}^{T} d\tau K(\tau)A(\tau)(\tau-T_0)=\psi^2(T), \tag{8}$$

$$B=2\psi(T_m), \tag{8a}$$

where $T_m=T(x=0)$ is the temperature on the energy-dissipation line.

From relation (8) with allowance for the boundary conditions (7) it is easy to obtain the temperature distribution in the SDS in implicit form:

$$x=\int_T^{T_m} d\tau K(\tau)/\psi(\tau). \tag{9}$$

Using relations (8) and (9) we can write for the effective length λ_T of the temperature change

$$\lambda_T=\frac{1}{T_m-T_0}\int_0^{\infty} dx[T(x)-T_0]=\frac{1}{T_m-T_0}\int_{T_0}^{T_m}\frac{d\tau K(\tau)(\tau-T_0)}{\psi(\tau)}. \qquad (10)$$

If $(T-T_0)\ll T_0$, expression (9) leads to an exponential decrease of the temperature with $\lambda_T=(K/A)^{1/2}$. This case, however, is of no great interest, since it can be realized only in the very narrow region where $T_0\approx T_c$. In all remaining cases, even at the minimum value of the voltage $V=2\Delta(T_m)/e$, the local superheat is of the order of T_0 itself. In this case λ_T depends substantially on the value of T_m determined from relation (8a), and as a rule exceeds $[K(T_0)/A(T_0)]^{1/2}$ by more than an order of magnitude. Estimates by formula (10) yielded λ_T of the order of 10^{-3} cm for all the investigated materials.

§3. Quantitative analysis of experimental data

It is of interest to compare the results of the calculations with the experimental data. To simplify the calculations we confine ourselves to the temperature interval $0.5T_c<T<T_c$, for which the functions $K(T)$ and $A(T)$ are given in Refs. 11–15. Substituting the corresponding expressions for $K(T)$ and $A(T)$ in (8), we obtain the connection of P with T_m and T_0:

$$P=R[3(T_m-T_0)^4+8(T_m-T_0)^3(T_0-0.5T_c)+6(T_m-T_0)^2(T_0-0.5T_c)^2]^{1/4}. \qquad (11)$$

In this formula, $R=(2/3)^{1/2}dW(K_0\gamma)^{1/2}$, $\gamma=A(T)/T^3$ is a constant, $K_0=4K_n(T_c)$, and $K_n(T_c)$ is the coefficient of the electronic thermal conductivity of the film in the normal state at $T=T_c$.

Using the estimates of H_1, H_2, and K_0 we find that for an indium film (sample 1) $R\sim10^{-4}$ W/K^2. It must be noted that the coefficient R can be estimated only roughly. It depends essentially on the film material, the sputtering conditions, the thermal properties of the ambient, etc., and can even vary noticeably from one section of the film to another. Nonetheless this coefficient can be calculated from (11) if we know for at least one value of $P=IV$ the exact value of T_m at the specified temperature T_m. It is useful in this connection to analyze the superconductivity destruction on the $I-T$ plane. To this end we show together in Fig. 4 a fragment of the CVC [Fig. 4(a)] and the corresponding trajectory on the $I-T$ plane [Fig. 4(b)]. Also shown on this plane is the experimental plot of $I_c(T)$, and in arbitrary form the dependence of the pair-breaking current I_p on the temperature [in the scale employed, $I_p(T)$ is almost a vertical line]. When the current goes from zero to I_M the temperature of the selected SDS remains constant at T_0. At the current I_M, a voltage jump takes place and the temperature increases jumpwise [see Fig. 4(b)], with formation of a normal region. The section HP on Fig. 4(b) is drawn arbitrarily in the form of a straight line. It is obvious that in the general case we have here a certain monotonic line that deviates from a straight line towards the T axis. On the section HQ, the calculated points (see below) lie on a straight line. The curve $I_c(T)$ bounds from above the region of the existence of a superconducting state at any initial T_0. In Fig. 4(b) this region is marked SS. The $I_p(T)$ curve and the axis section $T\geqslant T_c$ bound from below the region of existence of the normal strip in the SDS [this region is marked NS on Fig. 4(b)]. The point Q is the one at which the coefficient R of (11) can be determined. In fact, from the experimental $I_c(T)$ curve one determines $T_m=T_{mQ}$ from the known current $I_R=I_Q$. From the CVC of Fig. 4(a), in turn, we obtain the voltage and hence the power P_Q. Knowing R, we can obtain T_m for any point of the CVC in the vicinity of the MSDS where the approximation under which (11) was derived are valid.

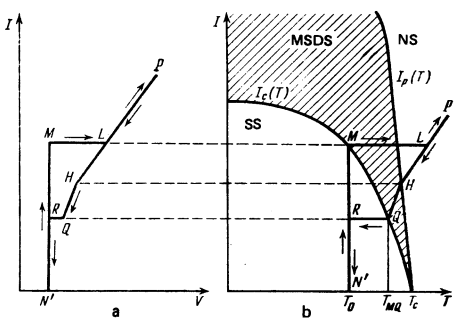

FIG. 4. $I-T$ diagram together with trajectory of the state of the film. The left side of the figure shows the corresponding CVC fragment.

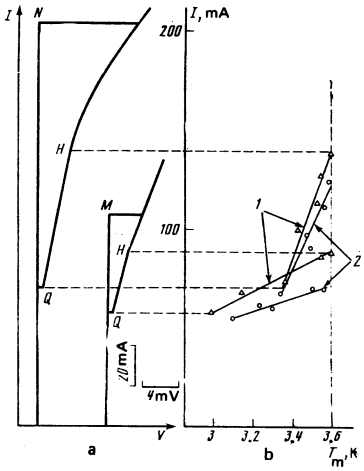

FIG. 5. Plot of $I(T_m)$ (b) for In film (sample 1), obtained from the corresponding CVC fragments (a) for two different temperatures. T_0: 1) 2 K, 2) 2.6 K.

Figure 5(a) shows the first and second fragments of the CVC of an indium film (sample 1) at $T_0=2$ K. To each point of these fragments corresponds a maximum temperature T_m in the SDS [Fig. 5(b)]. Curves 1 correspond to $T_0=2$ K, and curves 2 to $T_0=2.6$ K. The values of the coefficient R ($R_{1,2}$) for different sections of the film, determined from the CVC of these fragments, agree in order of magnitude with the estimate given above: $R_1=0.2\times10^{-4}$ and $R_2=0.6\times10^{-4}$ W/K^2.

Knowing T_m from (9), we can determine the temperature at any point x near the SDS.

The presented calculation of T_m presupposes that the hysteresis is determined completely by the heating of the SDS, inasmuch as for a given T_0 the value of T_{mQ} is uniquely determined by the value of the current hysteresis. To check on this assumption we used the CVC of a section of a film for ten different values of T_0 from

TABLE II. Comparison of experimental and calculated values of the current of the transition of Sn film (sample 47) from the metastable dissipative state to the superconducting state.

n	I_Q^{exp}, mA	I_Q^{calc}, mA	P_Q, mV	T_0, K	n	I_Q^{exp}, mA	I_Q^{calc}, mA	P_Q, mV	T_0, K
1	0.88	0.855	0.862	2.15	6	0.627	0.64	0.56	3.0
2	0.87	0.845	0.85	2.2	7	0.53	0.555	0.44	3.2
3	0.82	0.805	0.8	2.4	8	0.41	0.41	0.28	3.4
4	0.775	0.765	0.74	2.6	9	0.24	0.25	0.1	3.6
5	0.708	0.701	0.67	2.8	10	0.04	0.04	0.003	3.8

$0.5T_c$ to $0.98T_c$. For $T_0 = 0.5T_c$ the coefficient R was determined from the formula

$$\sqrt{3}R = P_Q(T_{mQ} - 0.5\ T_c)^{-2}.$$

For all other T_0, the value of T_{mQ} was determined from the measured P using formula (11). Along the trajectory on the $I-T$ plane, to each pair T_{mQ} and T_0 was set in one-to-one correspondence a superconducting transition current I_Q^{calc}. It was compared with the analogous value I_Q^{exp} measured from the corresponding CVC fragment. The best agreement between the currents was observed for a thin tin film (sample 47, see Table II). For Al (sample 23) and In (sample 1) films, the difference did not exceed 16%. It is important to note a calculation performed for values of K and A independent of T yielded no correlation whatever between I_Q^{calc} and I_Q^{exp}.

We note in conclusion that the behavior of all the samples fitted qualitatively the scheme considered here quite well. Not all of them, however, were in so good an agreement as those cited in the article. In those cases, however, when the quantitative discrepancy was substantial, it could always be attributed to one of the following factors. In sufficiently pure samples, the localization length of the electric field becomes of the order of the thermal length. On the other hand, in very dirty samples (such as granulated films), Eq. (11) no longer holds, and $K(T)$ and $A(T)$ were not measured as yet for such cases.

Thus, in all the parameter ranges where there is sufficiently complete information on the corresponding physical quantities and where the condition $l \ll \lambda_T$ is satisfied, the agreement between theory and experiment is always very good.

The authors thank A. A. Galkin for constant interest and support.

[1)]For type-I superconductors, $N = N\Phi_0/c\tau_L(I)$, where N is the number of flux quanta contained in one flux tube. All the arguments presented below for a type-II superconductor pertain also to type-I superconductors, with the term "vortex" replaced by "flux tube" and with Φ_0 replaced by $N\Phi_0$. The long range action for vortices is due to interaction through empty space, and remains in force therefore also for flux tubes.

[2)]Strictly speaking, this relation is valid only near T_c. It is clear, however, that the order of magnitude of l_E is determined by the length l_ε if $T < T_c$. There are also experimental data favoring this statement.

[3)]l_e is determined from the sample resistivity in the normal state at $T = 4.2$ K.

[1]V. L. Ginzburg, Dokl. Akad. Nauk SSSR **118**, 464 (1958) [Sov. Phys. Dokl. **3**, 102 (1958)].
[2]A. A. Galkin, Yu. M. Ivanchenko, and V. F. Khirnyĭ, Fiz. Tverd. Tela (Leningrad) **20**, 1237 (1978) [Sov. Phys. Solid State **20**, 713 (1978)].
[3]Yu. M. Ivanchenko and V. F. Khirnyĭ, Fiz. Nizk. Temp. **4**, 969 (1978) [Sov. J. Low Temp. Phys. **4**, 456 (1978)].
[4]Yu. M. Ivanchenko, V. F. Khirnyĭ, and P. N. Mikheenko, Zh. Eksp. Teor. Fiz. **77**, 952 (1979) [Sov. Phys. JETP **50**, 479 (1979)].
[5]W. C. Overteon, Jr., J. Low Temp. Phys. **5**, 397 (1971).
[6]J. Pearl, Appl. Phys. Lett. **5**, 65 (1964).
[7]J. Bardeen and J. R. Schrieffer, Progr. in Low Temp. Phys., Vol. III, NY, 1961 [Russ. transl. Fizmatgiz, 1962, p. 43].
[8]T. Y. Hsiang and J. Clarke, Phys. Rev. B21, 945 (1980).
[9]S. N. Artemenko and A. F. Volkov, Zh. Eksp. Teor. Fiz. **70**, 1051 (1976); **72**, 1018 (1977) [Sov. Phys. JETP **43**, 548 (1976); **45**, 533 (1972)].
[10]A. A. Maradudin, E. W. Montroll, and G. H. Weiss, Theory of Lattice Dynamics in the Harmonic Approximation, Academic, 1963 [Russ. transl. Mir, 1965, p. 315].
[11]W. J. Skocpol, M. R. Beasley, and M. Tinkham, J. Appl. Phys. **45**, 4054 (1974).
[12]D. A. Neeper and J. R. Dillinger, Phys. Rev. **A135**, 1028 (1964).
[13]J. J. Gittelman and S. Bozowski, Phys. Rev. **128**, 646 (1962).
[14]V. G. Volotskaya, A. Bogdzevich, L. E. Musienko, and Yu. V. Kalekin, Cryogenics **18**, 557 (1978).
[15]C. B. Satterthwaite, Phys. Rev. **125**, 873 (1962).

Translated by J. G. Adashko